Check for updates

Methanol production in a sustainable, mild and competitive process: concept launch and analysis†

Phillip Nathrath, [iD] [a] Fabian Kroll, [iD] [b] David Karmann,[b] Michael Geißelbrecht [iD] [b] and Patrick Schühle [iD] *[a]

In this study, we propose a novel process route for the conversion of wet biomass into renewable methanol under unprecedentedly mild reaction conditions, that operates at pressures below 10 bar and temperatures around 200 °C. Unlike conventional thermochemical routes, which require extreme conditions and complex processing steps, our approach follows a previously unexplored pathway *via* the intermediates formic acid and methyl formate, achieving high single-pass methanol yields. This process offers remarkable flexibility regarding biomass feedstock and is particularly well suited for decentralized applications. By integrating biomass valorization with hydrogen and oxygen from water electrolysis, the need for fossil-based reactants is eliminated, enhancing both sustainability and scalability. A techno-economic assessment demonstrates a high carbon efficiency of 80.0% and competitive methanol production costs between 0.69 and 2.31 € per kg, depending on the scenario. Although still in the early stages of development, the process offers carbon and energy efficiency comparable to biomass gasification- and power-to-methanol technologies, while showing strong potential for further advancement towards practical application and to effectively complement future sustainable methanol production.

Green foundation

1. In our research, we developed a novel process route that could be a game changer for sustainable methanol production from biomass, as it operates under mild process conditions and reduces the need for prior biomass drying and intensive product purification. This route complements the transition from fossil to renewable methanol synthesis and could even outperform sustainable alternatives based on harsh gasification and expensive power-to-X technologies.

2. The proposed route yields a superior single-pass carbon efficiency of >80% under mild conditions, with the option to integrate an electrolyser for a fully decentralized and autonomous system. Since biomass typically accumulates in decentralized locations, the new process can be implemented close to these sources, minimizing feed transport distances and further reducing greenhouse gas emissions.

3. In future work, the interaction of the concept sub-processes should be demonstrated experimentally in a real-life scenario.

1. Introduction

Methanol plays a crucial role as a versatile base chemical and a promising energy carrier and fuel.[1,2] It serves as a key feedstock in the production of formaldehyde, methyl *tert*-butyl ether (MTBE), acetic acid, and a wide range of polymers, while its potential as a liquid fuel and hydrogen carrier positions it as a vital component in future sustainable energy systems.[3] As global efforts to decarbonize industrial sectors intensify, the demand for renewable methanol is expected to grow significantly.[4]

Today, methanol is predominantly produced *via* fossil-based processes, primarily using natural gas as the feedstock.[3] This conventional route, while well-established, is associated with significant greenhouse gas emissions, making it incompatible with long-term climate goals. To address this, various renewable methanol production technologies have been developed or are under exploration, aiming to reduce the environmental footprint of this essential chemical.[5,6]

Two prominent pathways for renewable methanol production are power-to-X (PtX) and biomass gasification. The PtX approach combines carbon dioxide captured from industrial or atmospheric sources with green hydrogen generated through water electrolysis powered by renewable electricity. These reactants are subsequently converted into methanol in a high-pressure reaction, which is strongly limited by thermodynamic equilibrium, posing significant efficiency challenges. While recent advances in catalytic and electrochemical strat-

[a]Lehrstuhl für Chemische Reaktionstechnik, Friedrich-Alexander-Universität Erlangen-Nürnberg, 91058 Erlangen, Germany. E-mail: Patrick.Schuehle@fau.de
[b]Forschungszentrum Jülich GmbH, Helmholtz Institute Erlangen-Nürnberg for Renewable Energy, 91058 Erlangen, Germany
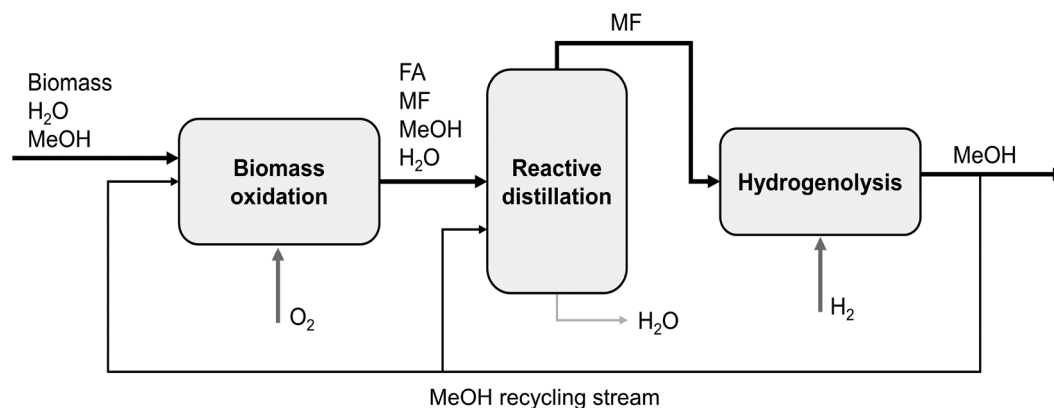†Electronic supplementary information (ESI) available. See DOI: https://doi.org/10.1039/d5gc01307k

Fig. 1 Flowsheet of the novel process route for methanol production from wet biomass (OxFA-to-MeOH process; flowsheet showing only major components (>5 wt%) of the stream). MF: methyl formate, MeOH: methanol, FA: formic acid.

egies, such as CO_2-to-methanol synthesis *via* formic acid intermediates, have been proposed to circumvent these limitations, their practical viability remains uncertain.[7] Although the use of ionic liquids as promoters has shown promise in laboratory settings by enhancing reaction rates and selectivity, and process simulations suggest potential scalability, these approaches still require further research.[8,9] The complexity of multi-step reduction pathways, potential catalyst deactivation, and additional costs of ionic liquids need to be considered with regard to large-scale deployment. Biomass gasification, on the other hand, converts a wide range of biomass including lignocellulosic residues into syngas, which can then be synthesized into methanol. Here, all subprocesses are already established in large scale and preprocessing of the biomass is essentially limited to drying, grinding and classification or pelletization without chemical pretreatment. However, biomass gasification is often constrained by the harsh operation conditions, high capital costs, process inefficiencies related to gas cleaning and conditioning and complexity of feedstock logistics.[10,11] The latter resulting from low volumetric energy density of biomass, that is produced locally and challenging to transport efficiently without any preprocessing steps like pelletation.[12,13] This disparity drives demand for decentralized biomass-to-methanol conversion technologies, strategically distributing production facilities closer to biomass sources.

To address these challenges, we propose a novel process for methanol production from wet biomass residues *via* the intermediate formic acid under overall mild reaction conditions (OxFA-to-MeOH process), making it attractive for decentral biomass conversion.

Fig. 1 provides an overview of the proposed OxFA-to-MeOH process route for methanol synthesis from biomass residues. Each process step will be described in detail below.

1.1 Biomass oxidation (OxFA process)

The OxFA process represents a promising technology for the selective oxidation of various biomass feedstocks with oxygen to produce formic acid. Currently under commercial develop-

ment by OxFA GmbH, this process has the potential to contribute to the state-of-the-art production of formic acid in the future.[14] The process was first introduced by Albert *et al.* employing a Keggin-type polyoxometalate (POM) as a homogeneous catalyst.[15] Here, formic acid yields of up to 53% were reached at 30 bar oxygen pressure and 90 °C and xylan as feedstock. In addition to mono- and disaccharides as well as crude glycerol various complex, water-insoluble biomass residues, such as pomace, grass clippings, wood chips or straw, could be converted when they are combined with efficient promoters (*e.g.* *p*-toluenesulfonic acid, TSA).[16–18] Albert *et al.* also describe the conversion of contaminated feedstock like effluent or deinking sludge, although high nitrogen contents or contamination with heavy metal cations (Pb^{2+} or Cu^{2+}) have a negative impact on the oxidation reaction.[17] Subsequent studies have focused on advancing the process further and exploring the underlying reaction mechanism in greater depth.[19–23] A main challenge of the OxFA process is the competing total oxidation of biogenic carbon to carbon dioxide, instead of formic acid, reducing the overall carbon efficiency of the process. In 2020 Maerten *et al.* showed that methanol as a solvent completely suppresses total oxidation.[24] Here, glucose was used as the model biomass substance and it was demonstrated that even with a small addition of methanol to an aqueous biomass solution (90 : 10 water : methanol), the formation of CO_2 is almost completely prevented (eqn (1) shows the partial oxidation of glucose to formic acid). The methanol in the solution leads to a faster reoxidation of the HPA-5 catalyst allowing the reaction to proceed efficiently at oxygen pressures as low as 5 bar. However, methanol and formic acid can be esterified in a subsequent reaction to form methyl formate according to eqn (2).

$$C_6H_{12}O_6 + 3O_2 \rightarrow 6CH_2O_2 \qquad (1)$$

$$CH_2O_2 + CH_3OH \rightleftharpoons C_2H_4O_2 + H_2O \qquad (2)$$
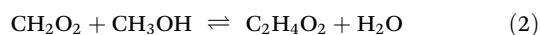
Due to the use of moist biomass, the solvent ratio of the methanol-modified OxFA process is usually in favor of water. According to the thermodynamic equilibrium of reaction (2),

this results in a high FA : MF product ratio at the reactor outlet.

Both OxFA processes, utilizing purely aqueous and methanol-additised solutions, have already been investigated for potential industrial applications. Albert *et al.* explored the aqueous OxFA process as a foundation for hydrocarbon production *via* Fischer–Tropsch synthesis, while Kroll *et al.* conducted a techno-economic analysis of hydrogen production based on the methanolic OxFA process and formic acid dehydrogenation.[25,26] Due to the moderate operating conditions, with temperatures below 100 °C, pressures below 10 bar, and the use of air as an oxidizer, this reaction is highly suitable for decentralized implementation.

1.2 Reactive distillation

In the reactive distillation step, the formic acid from the OxFA process is intended to be completely converted to methyl formate according to eqn (2). The esterification is an exothermic equilibrium reaction for which both homogeneous and heterogeneous catalysts have been investigated. As homogeneous Brønsted acidic catalysts, H_2SO_4, HCl, HI, and *p*-toluene sulfonic acid are commonly used, with H_2SO_4 being the most widely employed one.[27] The main disadvantages of these mineral acids are their high corrosiveness, toxicity, and difficulties in separation. These characteristics often result in disposal costs that exceed the costs of raw materials, making them also environmentally undesirable.[28] A good alternative are solid acid catalysts (SACs), in which acidic groups are bound to a solid support using a physical or chemical method.[29] Examples of such SACs are zeolites, heteropolyacids, ion exchange resin or supported chlorides.[30–33] The conversion of formic acid and methanol to methyl formate and water is limited by the thermodynamic equilibrium of the esterification reaction. To reach nearly full conversion, the volatile product methyl formate can be separated *in situ*, using a reactive distillation setup. Therein, methyl formate is extracted in the head, whereas water and unreacted formic acid remains in the bottom. The boiling points of the chemicals involved are given in Table 1.

Orjuela *et al.* experimentally investigated esterification using reactive distillation in their study.[35] Conversions of up to 100% were achieved using Amberlyst 70. The continuous separation of MF through the column trays favors the shift of the equilibrium to the product side. Other groups have shown that also Amberlyst 15 and 36 are effective catalysts for esterification reactions.[36,37] Another advantage of reactive distillation is its ability to prevent the formation of the azeotrope between formic acid and water, which would otherwise form in the lower section of the column.[38] This is achieved through the reaction of formic acid with methanol beyond the azeotropic point.[39]

1.3 Hydrogenolysis

In a final process step, methyl formate converted to two molecules of methanol *via* exothermic hydrogenolysis using renewable hydrogen (eqn (3)).

$$C_2H_4O_2 + H_2 \rightleftharpoons 2CH_3OH \qquad (3)$$
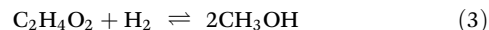
According to Le Chatelier, low temperatures and high pressures are advantageous for this reaction, what also suppresses the formation of potential byproducts (*e.g.*, dimethyl ether, carbon monoxide or methane).[40] Heterogeneous catalysts such as palladium or ruthenium supported on Al_2O_3 and SiO_2 have been studied for MF hydrogenolysis.[41,42] Due to their availability and lower cost, copper catalysts provide advantages over precious metals. Cu/SiO_2 and $CuO/ZnO/Al_2O_3$ have demonstrated good stability and selectivity.[43–45] While Monti *et al.* observed a reversible deactivation of Cu/SiO_2 at CO concentrations above 1–2% (coming from competing MF decarbonylation), Wu *et al.* reported no deactivation of their Cu/SiO_2 system over 250 h on stream.[43,44] Haagen *et al.* investigated $Cu_{0.9}Al_2O_4$ spinel catalysts, which exhibited excellent selectivity and stability over 110 h on stream, even with FA impurities in the feed stream.[46] The results further demonstrate that the hydrogenolysis of methyl formate can be carried out in both liquid and gas phases, although the reaction has yet to be commercially implemented. Utilizing a gas-phase reaction offers the advantage of operating at lower pressures. The typical operating conditions involve temperatures ranging from 150 to 250 °C and pressures below 25 bar.

2. Materials and methods

2.1 Simulation

The OxFA-to-MeOH process was simulated using Aspen Plus and optimized for a feed rate of 1 kmol h⁻¹ glucose (equals 180.2 kg h⁻¹). The thermodynamic model UNIQUAC was chosen to precisely model the interactions between the compounds in the simulation. Non-condensable gases (CO_2, O_2, and H_2) were defined as Henry components. The flow diagram within the simulation environment is provided in the ESI Fig. S1.† Each process step was simulated using specific reactor models tailored to the reactions and assumed conditions (compare ESI Tables S1 and S2†). Table 2 summarizes the main assumptions used for the simulation in Aspen Plus.

The sensitivity analysis included the addition of an alkaline water electrolyzer. The carbon efficiency η_c was calculated using the following equation:

$$\eta_c = \frac{\dot{n}_{MeOH, out}}{\dot{n}_{glucose, in} \cdot 6} \times 100\% \qquad (4)$$

The energy analysis was performed using the integrated Aspen Energy Analyzer. This included a pinch analysis to identify potential heat exchanger networks, allowing the

Table 1 Boiling points of the compounds in the reactive distillation at 1 bar[34]

	Formic acid	Water	Methanol	Methyl formate
Boiling point	100.8 °C	100.0 °C	64.7 °C	31.5 °C

Table 2 Overview of core assumptions for the process simulation

Block/stream	Parameter	Value	Unit
Feed	Methanol content (solution)	10	%
Biomass oxidation	Conversion	99	%
	Selectivity	98	%
	Temperature	90	°C
	Oxygen pressure	5	bar
Reactive distillation	Conversion	Equilibrium	—
Hydrogenolysis	Conversion	95.3	%
	Selectivity	100	%
	Temperature	210	°C
	Pressure	10	bar
Condenser	Temperature	25	°C
Split	Recycle to biomass oxidation	0.624	kmol h^{-1}
	Recycle to distillation	5.5	kmol h^{-1}

optimal network configuration to be implemented in the simulation. The overall energy efficiency η_e of the process is defined as the ratio of total energy in the methanol product stream on basis of the lower heating value, divided by the sum of energy inputs (electricity, biomass, heat):

$$\eta_e = \frac{\sum \dot{E}_{prod}}{\sum \dot{E}_{in}} = \frac{\dot{m}_{MeOH,out} \cdot LHV_{MeOH}}{\sum \dot{E}_{in}} \times 100\%. \quad (5)$$

2.2 Cost estimation

For cost estimation, both capital expenditure (CapEx) and operational expenditure (OpEx) were calculated. CapEx was determined using the Aspen Process Economic Analyzer, which applies a volumetric estimation method. For all components with contact to chemical streams stainless steel is considered as material of choice. As the software provides results in USD, a conversion rate of 0.9 € per USD was applied.[47] Assuming a standard amortization period of 20 years, the annual cost of methanol production includes a 5% charge from the CapEx.

In calculating OpEx, only energy and material costs of the process steps in Fig. 1 were considered, while other operational expenses, such as catalysts, product purification, labor, and maintenance, were excluded. A uniform price was applied for energy, not distinguishing between heating or cooling requirements (temperature, pressure). The assumed costs for the resources can be found in Table 3 and represent the base case of this study. The prices for hydrogen and oxygen refer to an external supply.

These prices are based on Germany as the proposed location and assume the utilization of green hydrogen to enable a renewable process. The simulated process is designed to operate for 8000 hours per year, allowing one month of downtime for maintenance and repairs. The minimum pro-

Table 3 Cost assumptions for operational expenditures (OpEx) in the base case

	Unit	Price	Source
Glucose	€ per kg	0.41	48
Water	€ per kg	0.001	49
Hydrogen (H$_2$)	€ per kg	4.89	50
Oxygen (O$_2$)	€ per kg	0.14	26
Heating	€ per kWh	0.067	51
Cooling	€ per kWh	0.005	52
Electricity	€ per kWh	0.20	53

duction costs of methanol in € are subsequently calculated using eqn (6).

$$C_{MeOH} = \frac{CapEx + OpEx}{\dot{m}_{MeOH,out}} \quad (6)$$

To reflect different feedstocks in the cost calculations we implemented a biomass price per glucose equivalent according to eqn (7) based on the carbon content of the gross biomass including ash and moisture $\omega_{C,am}$.

$$Price_{GE}(biomass) = \frac{\omega_C(glucose)}{\omega_{C,am}(biomass)} \times price(biomass) \quad (7)$$

3. Results and discussion

3.1 Simulation of the process

The biomass oxidation is realized in the modified OxFA process at 90 °C and 5 bar oxygen atmosphere using glucose as model substance. Here, a 10 wt% mixture of methanol in water is used as a solvent to suppress CO$_2$ formation.[24] It is assumed that the glucose concentration is applied close to its solubility equilibrium (47.4 wt% glucose). Aside from the partial oxidation of glucose to formic acid (FA), the total oxidation to CO$_2$ is considered as only side reaction. Based on published experimental data, a glucose conversion of 99% and a high selectivity to FA and MF of 98% is assumed for the modified OxFA process.[24,54] A detailed description of the simulated input and output flows can be found in Table S3.† For the reactive distillation step a column with 15 stages (13 reaction stages plus condenser and evaporator) is used to assure a high conversion of FA and a high purity of the removed MF. Methanol is added to the unit *via* a recycling stream on tray 8 as well as *via* the product mixture from the biomass oxidation step. The resulting temperature and composition profiles can be presented in Fig. S3.† A stream mainly consisting of water (94 wt%) and some residues of FA and methanol is withdrawn at the bottom of the column. Due to the low boiling point MF is separated at the head of the column, resulting in a condensate stream with approximately 98 wt% MF-content. Despite the high purity of the flow exiting the column some impurity buildup from recycling may still occur. Our study primarily assesses the basic feasibility, cost-effectiveness, and sustain-

ability of the process to determine if larger-scale experiments are justified. Definitive conclusions about impurity accumulation require experimental studies on higher technology readiness level (TRL). In the third step the MF-rich condensed head stream and hydrogen are feed into the hydrogenolysis reactor that operates at 210 °C and 10 bar.[46] Based on literature a high MF-conversion of 95.3% and no side reactions are assumed.[44] Further increase in reaction temperature can lead to higher conversions at the cost of selectivity and is therefore not considered.[46] Finally, the produced methanol-rich stream from MF hydrogenolysis is condensed at 25 °C. Roughly, 52% of this condensed stream is recycled and fed into the reactive distillation column and to a smaller extend to the glucose oxidation step. Consequently, the resulting net product stream is 158.9 kg h^{-1} with a methanol content of 96.7 wt% (pure methanol stream of 153.6 kg h^{-1}).

An in-depth view of the carbon balance of the described OxFA-to-MeOH process route can be derived from the Sankey-diagram shown in Fig. 2.

The overall carbon efficiency (CE) of the process route is 80.0%. In glucose oxidation 1.9 kg h^{-1} CO_2 are formed *via* the total oxidation path, representing a carbon loss smaller than 0.4%. The main carbon losses in the proposed process route are found in the reactive distillation step where FA and MeOH impurities in the aqueous bottom stream are the major contributors with only minor losses of uncondensed product in the head condenser unit. An increase of the separation efficiency, *e.g.* by lowering the cooling temperature or increasing the heat exchange surface in both condensing steps could lead to an overall increase in carbon efficiency at the cost of higher equipment or operation costs. A variation of the cooling temperature of the final product condenser can be found in Fig. S5.† Here, the reduction of the coolant temperature from initial 25 °C to 5 °C would result in a higher CE of 83.2%.

Both, glucose oxidation and hydrogenolysis are exothermal reactions. Consequently, there is a heat surplus in the considered process route. Due to the low reaction temperature in the oxidation reaction only the excess heat of the hydrogenolysis and the final product condensation steps is applicable for heat integration. The heat integration network generated with the Aspen Energy Analyzer is illustrated in Fig. S2† and consists of four heat exchangers offering a total heat exchange capacity of 183 kW. By using this surplus, the original heat demand of the process can be reduced by 96.1% from 190.1 kW to 7.3 kW and the demand for cooling is lowered by 25.8% from 707.7 kW to 524.9 kW. As the main amount of heat is produced in the glucose oxidation an increase of the reaction temperature beyond 100 °C could, however, enable the generation of valuable low-pressure saturated steam and thus the integration of the process into a local or district heating network, enhancing its economic viability. However, the effects of the higher temperature on the OxFA process performance would need to be investigated experimentally.

To estimate the environmental impact of the OxFA-to-MeOH process we calculated the GWP$_{100}$ (global warming potential over 100 years). The system boundaries (gate-to-gate) are visualized in Fig. 3a and the results for the base case and for additional flue gas combustion are shown in Fig. 3b. The underlying assumptions for the GWP$_{100}$ calculation can be found in the ESI section S.4.† In the base case 0.959 kg$_{CO_2\text{-eq}}$ kg$_{MeOH}^{-1}$ is emitted. The main contribution to this value are the emitted MF and H$_2$ gas streams from reactive distillation and from the product condenser, as both molecules obsess a relatively high GWP$_{100}$-value of 11 kg$_{CO_2\text{-eq}}$ kg$_{MF}^{-1}$ (MF) and 11.6 kg$_{CO_2\text{-eq}}$ kg$_{H_2}^{-1}$ (H$_2$). Therefore, we considered a second scenario where the flue gases are simply combusted to biogenic CO_2 resulting in significant reduction of the processes GWP$_{100}$ to 0.464 kg$_{CO_2\text{-eq}}$ kg$_{MeOH}^{-1}$. Additionally to the biogenic CO_2 as a value product in itself, the combustion would produce around 0.98 kWh kg$_{MeOH}^{-1}$ excess heat usable for other processes. Based on these results we conclude, that flue gas combustion would be an interesting option to further reduce the GHG potential of the OxFA-to-MeOH process, especially if the separation efficiency of MF and H$_2$ can not be improved.

3.2 Cost calculations for the base case

Following the simulation results, the CapEx for the base case of the OxFA-to-MeOH process can be calculated. A detailed listing of the costs for of all main components of the system is
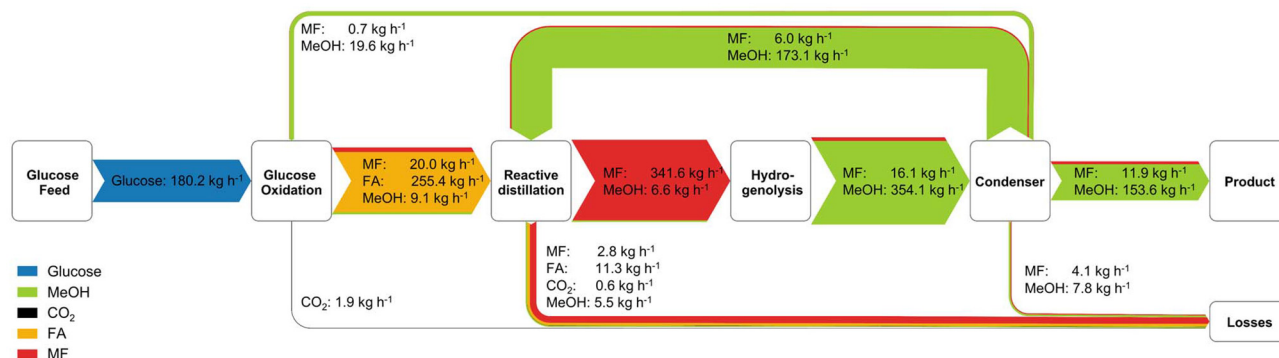

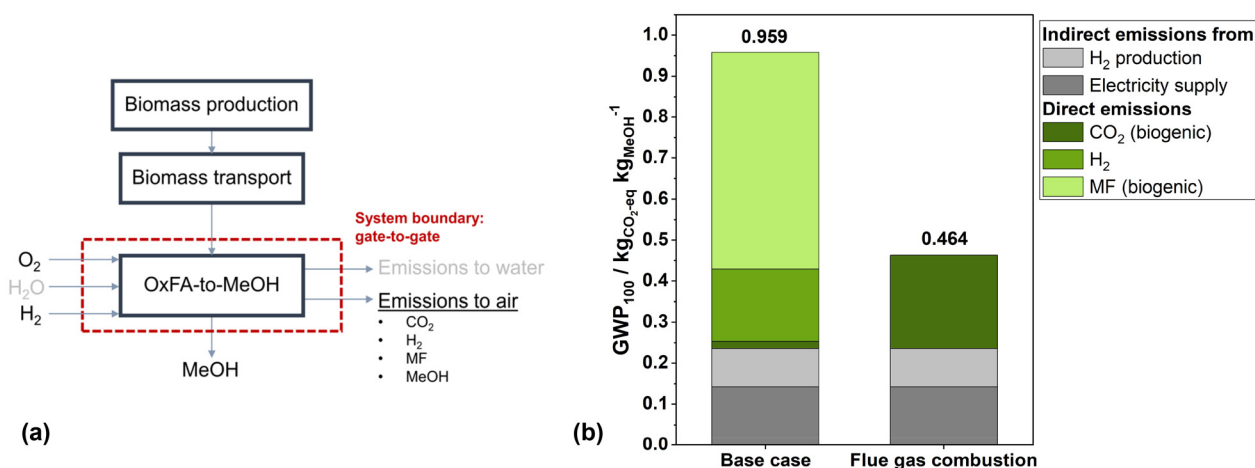**Fig. 2** Sankey diagram of the simulated process route with total CE of 80.0%.

Fig. 3 Environmental assessment of the OxFA-to-MeOH process: (a) system boundary visualization, (b) comparison of GWP_{100} of the base case and base case with flue gas combustion.

shown in Table S4.† In total 3.36 Mio.€ are necessary for the components including installation costs. Following the annual operation time of 8000 h a^{-1} over the 20 years amortization period this equals 21.01 € per h. Fig. 4(a) illustrates the relative amounts of the CapEx for each component.

The compressors for hydrogen and oxygen, followed by the reactive distillation column, cause the biggest impact on CapEx. Both, the OxFA reactor for the glucose oxidation (stirred tank reactor), as well as the hydrogenolysis reactor (tubular reactor) represent rather standard reaction equipment and hence have only moderate impact on CapEx. The lowest contribution to CapEx originates from the process equipment e.g. pumps, preheaters, heat exchangers and the product condenser.

Based on the assumptions in Table 3 the OpEx can be calculated as 217.26 € per h for the base case. Based on the methanol fraction of the product stream and the sum of CapEx and OpEx a (crude) methanol price of 1.55 € per kg is calculated. After amortization of the plant and equipment the methanol price lowers to 1.41 € per kg (see Fig. S4†). An overview of the relative distribution of the OpEx is given in Fig. 4(b), whereas the specified values for each item are summarized in Table S5.† The greatest cost impact arises from the renewable hydrogen and the biomass source glucose. Together they account for 88.2% of the OpEx (see Table 3). Accordingly,

these two factors have also the highest cost impact in the sensitivity analysis, as shown in Fig. 5. Note, that the depicted variation of the glucose costs can also be taken as a proxy for the additional OpEx of a potential pretreatment for complex biomass or higher base costs for the feed biomass.

The amortization period has a non-linear effect on the methanol price, which, however, is smaller than the impact of the price variation of hydrogen or glucose. In comparison the influence of CapEx, oxygen costs and electricity costs on the methanol price is low if varied in the same range of ±50%. Hence, the addition of suitable equipment for biomass pretreatment, e.g. an agitated steel basin (approx. 200.000 € CapEx), is well within the considered CapEx range, and would result in a minor increase of the methanol price from 1.55 to 1.56 € per kg. The variation of heating, cooling and water costs resulted in a negligible change of methanol price within a range of ±0.6% (see Table S6†).

3.3 Feedstock range expansion and integration potential for electrolysis

Glucose was chosen as the model substrate in the base case primarily due to the good availability of comprehensive published data. However, in a real application scenario, other biomass sources especially waste and residue streams are way
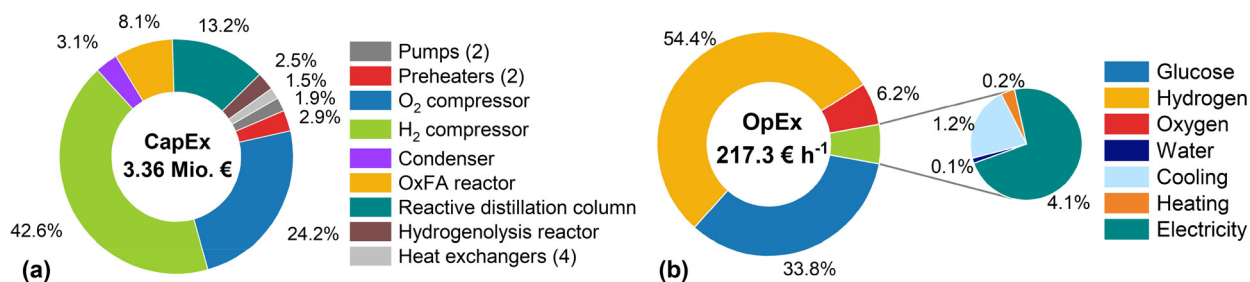

Fig. 4 Overview of CapEx (a) and OpEx (b) for the base case assumptions of the process route.
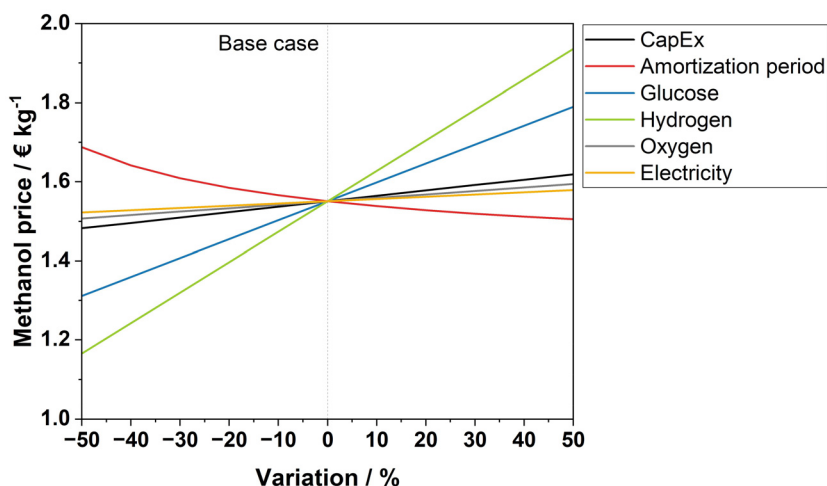
Fig. 5 Sensitivity analysis of the methanol price on a ±50% variation of the CapEx, amortization period, electricity price and feedstock costs (glucose, oxygen and hydrogen).

more attractive low-cost alternatives. Crude glycerol and wheat straw are two examples that have already been tested in the OxFA process and are feasible substrates for FA production.[17,18] As agricultural waste or residue of the bio diesel production, wheat straw or crude glycerol offer a high biomass potential and good availability in the region of Germany.[55,56] Other waste biomasses with high polysaccharide contents like pomace or sugar cane residues are potential carbon sources for the OxFA process, as well.[17] Due to their high sugar content with chemical similarity to glucose and low availability in Germany they are not considered as an extra case in this study. Table 4 summarizes the properties and costs of the three carbon sources evaluated in this study. Because the reaction is conducted in an aqueous environment, water, which is the main impurity in crude glycerol,[57] does not interfere with the process. Note, that the utilization of solid water insoluble lignocellulosic wastes, like wheat straw, requires the use of promotors (*e.g.* TSA) for effective conversion in the biomass oxidation step.[17] The costs for promotors and possibly additional pretreatment equipment (steel basin) is not accounted for in the current model, but is assumed within the range of the conducted sensitivity analysis (Fig. 5).

For wheat straw a moisture and ash content of 10.1 wt% and 6.4 wt% are assumed lowering the usable ash free dry

mass of the carbon source (mainly lignin, cellulose and hemi-cellulose) to approximately 83.5% of the gross weight.[58] This results in a C-content of the biomass including ash and moisture of 41.3 wt%. As consequence of the slightly higher C-content$_{am}$ compared to the reference glucose the price of wheat straw per glucose equivalent is calculated as 0.083 € per kg$_{GE}$. Note, that possible further losses during an eventually needed pretreatment of the biomass is not accounted for at this point. For crude glycerol on the other hand a purity of approximately 66.8 wt% is assumed. The main impurity in crude glycerol is water. Hence, no special pretreatment is required to utilize this carbon source for the process. The low purity of the crude glycerol reduces the C-content from 39.2 wt% (C-content$_{daf}$, pure glycerol) to 26.2 wt% (C-content$_{am}$). As a result of the lower C-content$_{am}$ of crude glycerol compared to glucose the price per glucose equivalent is calculated as 0.168 € per kg$_{GE}$.

The glucose equivalent prices (see Table 4), which factor in inorganic and water content of the biomass, are used to estimate the achievable methanol prices with the different feedstocks building on the base case calculations. In a first approximation, the conversion level for both alternative biomasses is kept constant (approx. 99%) and a direct conversion of complex biomass like wheat straw is assumed in the OxFA step of the process route. The resulting methanol prices are given in Fig. 6.

Starting from a methanol price of 1.55 € per kg with glucose the costs can be lowered to 1.27 € per kg using crude glycerol or even 1.17 € per kg using wheat straw as carbon source.

Apart from the biomass substrate renewable hydrogen for the hydrogenolysis reaction is a major cost driving factor (see Fig. 4(b)). As also oxygen is required for the process route the direct coupling with a water electrolyzer is an approach. Using Aspen Plus an 1.2 MW alkaline electrolyzer (AEL) was determined to be sufficient to supply hydrogen (12 kmol h^{-1}) and

Table 4 Overview of considered carbon sources for the simulated process route

Carbon source	$\omega_{C,daf}$/wt%	$\omega_{C,am}$/wt%	Price/€ per kg	Price$_{GE}$/€ per kg$_{GE}$
Glucose	40.0	40.0	0.410	—
Crude glycerol	39.2	26.2	0.110	0.168
Wheat straw	49.4 (ref. 58)	41.3 (ref. 58)	0.085[a]	0.083

daf, dry mass ash free. am, gross biomass including ash and moisture. GE, glucose equivalent. [a] Average from 08.2021–08.2024.[59]
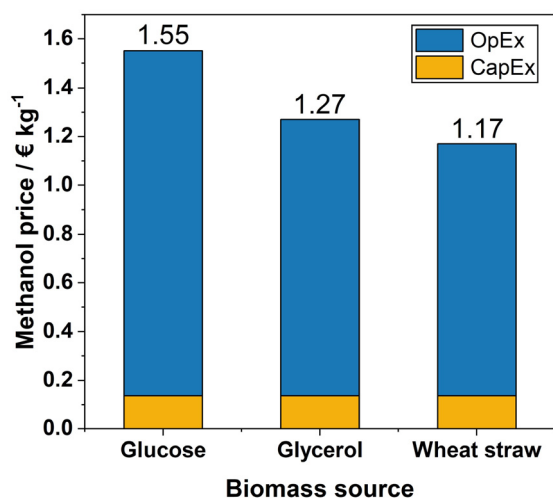
Fig. 6 Achieved methanol price in the base case scenario of the OxFA-to-MeOH process with different biomass as carbon source.

oxygen (3 kmol h^{-1}) for the full OxFA-to-MeOH process route. The excess oxygen might for example be used in waste water treatment or as growth agent in agriculture or aquaculture.[60–62] Under the assumption of 700 € per kW capital costs anticipated for small scale electrolyzers <5 MW in 2030 its implementation would increase the CapEx by an additional 0.84 Mio.€ to a total of 4.20 Mio.€.[63] Furthermore, the economic benefit of electrolyzer implementation highly depends on prevailing industrial electricity prices, as illustrated in Fig. 7.

Reaching an electricity price below 0.108 € per kWh, the use of an electrolyzer becomes economically viable. The current electricity production costs in Germany range from 0.041–0.144 € per kWh for photovoltaic and 0.043–0.103 € per kWh wind power and are therefore in a competitive range to run the process.[64] Note that depending on the use case the decentralized character of the in house production of hydrogen and oxygen can overweight the plain economic reasons even at higher electricity prices. For the applications in
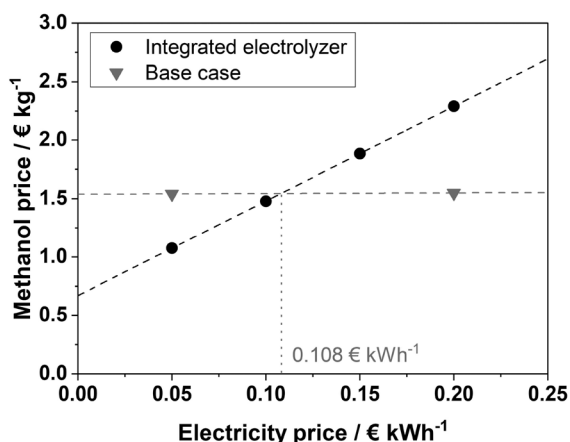

Fig. 7 Sensitivity analysis of the methanol price on electricity price.

Germany the electrolyzer integration can also be interesting for the combination with small-scale photovoltaic installations (<10 kW), since the feed-in remuneration (partial feed-in) for electricity from these sources is currently below 0.079 € per kWh.[65]

Furthermore, the integration of pressurized electrolyzer solutions might result in the redundancy of the hydrogen compressor, significantly reducing the CapEx of the process (compare Fig. 4).[66] With an electricity price of 0.05 € per kWh a methanol price of 1.08 € per kg can be achieved for the case being analyzed.

3.4 Case study for a small-scale and decentralized application of the process

Modular and flexible decentralized systems leverage foundational small-scale chemical process units to enable scalable, adaptable operations across diverse production volumes and market demands. A small scale realization the OxFA-to-MeOH process greatly benefits from the mild reaction conditions employed (temperature <210 °C, pressures <10 bar). Furthermore, the MF hydrogenolysis, unlike CO or CO_2 hydrogenation, is not constrained by equilibrium limitations. This eliminates the need for high-pressure gas recycling, that are especially difficult to realize in small scale operation.[67] Furthermore, the process circumvents the need for energy-intensive biomass drying, enabling the direct utilization of wet biomass. In contrast to high-temperature biomass conversion methods such as gasification, the formation of tars and chars is effectively avoided, thereby reducing downstream purification requirements. The integration of an electrolyzer, as discussed above, provides the option for an independent supply of hydrogen and oxygen on any location with sufficient renewable energy capabilities.

A potential decentralized application of the OxFA-to-MeOH process is its deployment within agricultural or forestry cooperatives, where locally sourced lignocellulosic wet biomass waste is converted to methanol for use as a fuel additive in their vehicle fleets.[68] Additionally, surplus heat generated during oxidation can be utilized for heating adjacent facilities.

In the following, we define three operation scenarios to investigate the cost structure of the decentral application of the OxFA-to-MeOH process route including the use of an electrolyzer. It is assumed that in all three cases the same amount of methanol as in the base case is supplied, and that cooling water is on hand. Moreover, the CapEx remains unchanged across the considered scenarios. All further assumptions can be found in the ESI.† The resulting methanol prices and their distribution are illustrated in Fig. 8.

In the optimistic scenario (Fig. 8(a)), electricity is available at a low price of 0.05 € per kWh and wheat straw is applied as a cheap carbon source. This leads to methanol prices as low as 0.69 € per kg. In addition to the necessity of low electricity costs, the conversion of complex biomass poses a challenge in this scenario. At the current state of research, complex biomass achieves lower conversions compared to glycerol and glucose.[17] However, pretreatment of the biomass or the use of

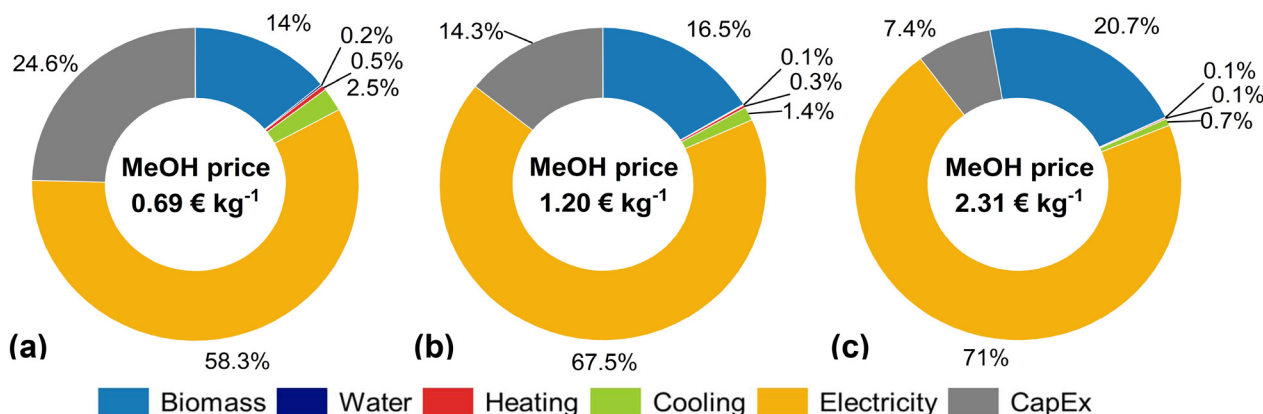| 14%	0.2%	16.5%	0.1%	20.7%	0.1%

Fig. 8 Results of the case study for the OxFA to methanol process route including the use of an electrolyzer (a) optimistic (b) neutral (c) pessimistic scenario.

additives can improve conversions.[15] Due to the high boiling points of these additives, they can be easily separated from the product mixture after the biomass oxidation step. In the neutral scenario (Fig. 8(b)) crude glycerol is the biomass in use, and electricity is provided at a price of 0.10 € per kWh, which is already achievable in some regions of Europe and could be feasible in Germany with the increase in renewable energy production.[64,69] Here, a methanol price of 1.20 € per kg is realized. In the pessimistic case in Fig. 8(c) a high electricity price of 0.20 € per kWh is assumed, and glucose is the only carbon source available. Hence, this scenario might be representative for the realization of the process at present time in Germany using a high-priced biomass source. With 2.31 € per kg the resulting methanol price is higher than in the base case assumptions described above. Consequently, for such a high electricity price, the OxFA-to-MeOH process route without the use of an electrolyzer is more economically viable. After amortization of the plant a methanol price of 2.14 € per kg can be achieved in the pessimistic scenario, whereas the neutral and optimistic cases reached methanol prices of 1.03 € per kg and 0.52 € per kg.

3.5 Comparison to other sustainable methanol production routes

The OxFA-to-MeOH process (optimistic scenario) proposed here has to compete against other sustainable methanol production routes, such as biomass gasification to methanol (BG-MeOH) or the direct conversion of CO_2 to methanol *via* PtX-technologies (E-MeOH). In Table 5 the main assumptions and key performance indicators (carbon efficiency, energy efficiency, TRL and methanol price) of the novel process route are contrasted against mentioned alternatives based on data from Harris *et al.*[70] In this study, the production of E-MeOH was simulated *via* the indirect process route namely by the electrocatalytic reduction of CO_2 to CO and subsequent methanol synthesis using H_2 from water electrolysis. For the BG-MeOH route, gasification is simulated at 1140.2 K and 243 kPa with combustion of the produced tars and chars as the primary heat source for the process. Excess CO_2 is removed to

about 5 vol% *via* acid-gas removal from the formed syngas before it is fed into the methanol synthesis reactor. To increase the comparability of the OxFA-to-MeOH process we recalculated the methanol price according to the assumptions and depreciation method (DCFROR – Discounted Cash Flow Rate of Return) used by Harris *et al.* This includes an internal return of revenue of 10% for the produced methanol.

Out of the three production processes the gasification route offers the lowest carbon efficiency of 33.2% due to high amounts of carbon lost in tars and chars that are combusted (approximately 31%).[70] The highest carbon efficiency of 91.5% can be achieved *via* the E-MeOH route. The primary carbon losses in this case are small slipstreams and separated side products (light hydrocarbons) both of which are utilized as process fuel. The OxFA-to-MeOH process also achieves a high carbon efficiency of 80.0%. Here, the main carbon losses arise from imperfect separation in the distillation and condensation steps. For comparison, conventional methanol synthesis pathways from fossil resources exhibit carbon efficiency in the range of 68–75%, what is below the here defined E-MeOH and OxFA-to-MeOH routes.[70]

The energy efficiency of the three production routes considered lies between 41 and 48%, with further improvement anticipated with increasing TRL for the E-MeOH and OxFA-to-MeOH routes. Therefore, all routes have a lower energy efficiency than current commercial methanol production, which averages 57%.[70] For the OxFA-to-MeOH route, a full utilization of the low-temperature waste heat could result in an increase of energy efficiencies up to 70% (when considering process heat as a product in eqn (5)). Due to the low requirements on the biomass feedstock (lignocellulosic wastes with variable composition, level of impurities and particle size) and high TRL (7–9) the methanol production by biomass gasification according to Harris *et al.* achieves the lowest methanol price of the routes considered.[70,73–75] With 0.35 € per kg it is within the range also reported by the International Renewable Energy Agency (IRENA) for bio based methanol production routes (0.29–0.69 € per kg; gasification, biogas reforming,

Table 5 Comparison of renewable methanol production routes (data for BG- and E-MeOH from Harris et al.[70])

Parameter	Unit	OxFA-to-MeOH		BG-MeOH	E-MeOH
Carbon source	—	Wheat straw		50% clean pine / 50% forest residues	CO_2
	€ per t	82.6		60.1	36.0
Electricity	€ per kWh	0.05	0.061	0.061	0.061
Plant life	a	20[a]	30	30	30
MeOH production	kt a^{-1}	1.21		291	291
Depreciation method	—	Amortization	DCFROR	DCFROR	DCFROR
Internal rate on return	%	—	10	10	10
Operation time	h a^{-1}	8000	7884	7884	7884
η_c	%	80.0		33.2	91.5
η_e	%	43.5		47.8	41.0
TRL[71]	—	4		7–9	4–8[b]
Methanol price	€ per kg	0.69	0.98	0.35	1.45

[a] Amortization period. [b] Depending on CO_2 source/direct air capture method.[7,72] DCFROR – discounted cash flow rate of return.

wood pulping) and even below the European market price of 0.50 € per kg for conventional methanol (averaged over the past three years 12.2021–12.2024).[4,76]

One major influence on the methanol price is the costs of the carbon source, which is assumed significantly cheaper in the BG-MeOH route of Harris et al. compared to the OxFA-to-MeOH process. In contrast, E-MeOH routes are more expensive than the two biomass based routes with methanol prices ranging from 1.08 to 2.16 € per kg for direct air capture solutions according to IRENA.[4] The E-MeOH price of 1.45 € per kg calculated by Harris et al. is in good agreement to these values and is approximately 48% higher than the price achieved in the OxFA-to-MeOH process under similar calculation assumptions (0.98 € per kg see Table 5). The high production costs of E-MeOH primarily stem from expensive renewable hydrogen and electricity. Furthermore, it can be noted, that the two processes in the study of Harris et al. are designed for significantly higher methanol production rates (factor 240) utilizing the advantages of economy of scale. One drawback of large plants and consequently high biomass throughput is the tremendous transport effort required, that is not considered in the study. Scaling down the E-MeOH and especially BG-MeOH processes might results in increasing methanol production costs in decentralized application scenarios.

The overall TRL for the OxFA-to-MeOH process was assigned as 4. While the biomass oxidation via the OxFA process possess a TRL of 7 and is currently implemented as pilot plant, the two subsequent processes esterification via reactive distillation and hydrogenolysis of MF are only realized at the laboratory scale.[27,46] In the presented case of E-MeOH (Harris et al.) the first step of electrocatalytic CO_2 reduction to CO has a low TRL of 4, the downstream syngas conditioning and methanol synthesis on the other hand are already established technologies with TRL 9.[70,77] Other routes such as the direct hydrogenation of CO_2 are also conceivable for the production of renewable methanol and reach up-to TRL 8 depending on the employed CO_2 source (point sources or direct air capture).[7,72] Consequently, it has to be denoted that the lower TRL of the OxFA-to-MeOH and E-MeOH routes are associated with increased risks related to process scalability and introduce uncertainties concerning the final commercial design. However, in the future the drastically higher carbon efficiency and therefore lower CO_2 emissions of the two processes could render them as promising alternatives to the conventional methanol production route, if renewable electricity prices decrease further or natural gas price increases further. Additionally, OxFA-to-MeOH opens the scope to a variety of wet biomass resources that cannot be used without prior energy-intensive drying in biomass gasification. Together with the decentralized nature of the concept, bio-methanol production via the proposed process route could convert biomass waste streams from farming associations producing methanol that can be sold or used as replacement fuel.[68]

4.   Conclusions

In summary, this study introduces a novel approach for the decentralized production of methanol from wet biomass residues (OxFA-to-MeOH process). First, biomass is oxidized with addition of methanol as solvent (approximately 10 wt%) via the modified OxFA process, generating formic acid in high yield. In the next step, the formic acid molecule is esterified with an additional molecule of methanol in a reactive distillation step, forming methyl formate. Lastly, the hydrogenolysis of methyl formate is carried out, forming two molecules of methanol. Roughly half of this high purity methanol product stream is recycled as reactant for the prior steps (OxFA process and esterification). The other half of the biogenic methanol is the product of the new process route.

The advantages of this concept are as follows: a wide variety of biomass sources (incl. residues and biogenic waste streams) can be used in the oxidation reaction without energy intensive pretreatment or drying steps. Together with the overall mild reaction conditions (<210 °C and <10 bar) this makes the concept feasible for small scale and decentral production of renewable methanol. In that way, extensive transport of low density biomass is avoided. In a future scenario, local suppli-

ers of biomass residues may use the produced methanol as fuel additive themselves.

The simulation results show that the proposed process chain achieves a high carbon efficiency of 80.0%, being superior to bio methanol from gasification and even current fossil methanol production routes. The novel route shows promising results for the integration of an alkaline electrolyzer to cover the inherent hydrogen and oxygen demand, if the prices for renewable electricity continue to fall. In the base scenario, where glucose is used as the biomass feedstock, the attainable methanol price of 1.51 € per kg is strongly influenced by the cost of renewable hydrogen. If an electrolyzer is used for the hydrogen supply the electricity price becomes the predominant influence for the methanol price resulting in a price range from 0.69–2.31 € per kg depending on the assumed scenario. In conclusion, the proposed methanol production route offers a decentralized approach in a competitive price range to other renewable methanol processes that either operate under challenging reaction conditions (biomass gasification) or rely on expensive CO_2 capture.

Conflicts of interest

There are no conflicts to declare.

Data availability

Data for this article are available at the data repository Zenodo at **https://doi.org/10.5281/zenodo.14679015**.

Acknowledgements

References

1 *Methanol: The Basic Chemical and Energy Feedstock of the Future: Asinger's Vision Today*, ed. M. Bertau, H. Offermanns, L. Plass, F. Schmidt and H.-J. Wernicke, Springer Berlin Heidelberg, Berlin, Heidelberg, 2014.

2 F. Schorn, J. L. Breuer, R. C. Samsun, T. Schnorbus, B. Heuser, R. Peters and D. Stolten, *Adv. Appl. Energy*, 2021, **3**, 100050.

3 F. Dalena, A. Senatore, A. Marino, A. Gordano, M. Basile and A. Basile, in *Methanol*, Elsevier, 2018, pp. 3–28.

4 S. Kang, F. Boshell, A. Goeppert, S. G. Prakash, I. Landälv and D. Saygin, *Innovation outlook: renewable methanol*, International Renewable Energy Agency, Abu Dhabi, 2021.

5 Z. Sun and M. Aziz, *J. Cleaner Prod.*, 2021, **321**, 129023.

6 S. Sollai, A. Porcu, V. Tola, F. Ferrara and A. Pettinau, *J. CO2 Util.*, 2023, **68**, 102345.

7 V. R. S. Alves and D. C. Meyer, *Rev. IPT: Tecnol. Inov.*, 2022, **6**, 6–36.

8 T. O. Bello, A. E. Bresciani, C. A. O. Nascimento and R. M. B. Alves, *Comput.-Aided Chem. Eng.*, 2022, **49**, 163–168.

9 T. O. Bello, A. E. Bresciani, C. A. O. Nascimento and R. M. B. Alves, *Chem. Eng. Sci.*, 2021, **242**, 116731.

10 H. B. Goyal, D. Seal and R. C. Saxena, *Renewable Sustainable Energy Rev.*, 2008, **12**, 504–517.

11 J. Hrbek, C. Pfeifer, P. Blanco-Sanchez, R. Baldwin, M. Swanson and J. Strege, *IEA Bioenergy*, 2025, 5–16.

12 V. Balan, *ISRN Biotechnol.*, 2014, **2014**, 1–31.

13 J. S. Tumuluru, C. Igathinathane, D. Archer and R. McCulloch, *Front. Energy Res.*, 2024, **12**, 1347581.

14 P. Preuster and J. Albert, *Energy Technol.*, 2018, **6**, 501–509.

15 J. Albert, R. Wölfel, A. Bösmann and P. Wasserscheid, *Energy Environ. Sci.*, 2012, **5**, 7956.

16 J. Albert, *Faraday Discuss.*, 2017, **202**, 99–109.

17 J. Albert and P. Wasserscheid, *Green Chem.*, 2015, **17**, 5164–5171.

18 R. Wölfel, N. Taccardi, A. Bösmann and P. Wasserscheid, *Green Chem.*, 2011, **13**, 2759.

19 J. Albert, D. Lüders, A. Bösmann, D. M. Guldi and P. Wasserscheid, *Green Chem.*, 2014, **16**, 226–237.

20 J. Albert, M. Mendt, M. Mozer and D. Voß, *Appl. Catal., A*, 2019, **570**, 262–270.

21 J. Reichert, B. Brunner, A. Jess, P. Wasserscheid and J. Albert, *Energy Environ. Sci.*, 2015, **8**, 2985–2990.

22 T. Lu, J. Wang, G. Wei, G. Li, Y. Wang, W. Wu and Y. Liang, *Fuel Process. Technol.*, 2022, **238**, 107493.

23 J. Reichert and J. Albert, *ACS Sustainable Chem. Eng.*, 2017, **5**, 7383–7392.

24 S. Maerten, C. Kumpidet, D. Voß, A. Bukowski, P. Wasserscheid and J. Albert, *Green Chem.*, 2020, **22**, 4311–4320.

25 J. Albert, A. Jess, C. Kern, F. Pöhlmann, K. Glowienka and P. Wasserscheid, *ACS Sustainable Chem. Eng.*, 2016, **4**, 5078–5086.

26 F. Kroll, M. Schörner, M. Schmidt, F. T. U. Kohler, J. Albert and P. Schühle, *Int. J. Hydrogen Energy*, 2024, **62**, 959–968.

27 Z. Khan, F. Javed, Z. Shamair, A. Hafeez, T. Fazal, A. Aslam, W. B. Zimmerman and F. Rehman, *J. Ind. Eng. Chem.*, 2021, **103**, 80–101.

28 P. Gupta and S. Paul, *Catal. Today*, 2014, **236**, 153–170.

29 C. M. Mendaros, A. W. Go, W. J. T. Nietes, B. E. J. O. Gollem and L. K. Cabatingan, *Renewable Energy*, 2020, **152**, 320–330.

30 E. G. Fawaz, D. A. Salam and T. J. Daou, *Microporous Mesoporous Mater.*, 2020, **294**, 109855.

31 E. Sert and F. S. Atalay, *Ind. Eng. Chem. Res.*, 2012, **51**, 6666–6671.

32 A. D. Buluklu, E. Sert, S. Karakuş and F. S. Atalay, *Int. J. Chem. Kinet.*, 2014, **46**, 197–205.

33 L. Di Bitonto, S. Menegatti and C. Pastore, *J. Cleaner Prod.*, 2019, **239**, 118122.

34 P. Linstrom, *NIST Chemistry WebBook, NIST Standard Reference Database Number 69*, ed. P. J. Linstrom and W. G. Mallard, National Institute of Standards and Technology, Gaithersburg MD, 1997, DOI: **10.18434/T4D303**.

35 A. Orjuela, A. Kolah, C. T. Lira and D. J. Miller, *Ind. Eng. Chem. Res.*, 2011, **50**, 9209–9220.

36 T. Pöpken, L. Götze and J. Gmehling, *Ind. Eng. Chem. Res.*, 2000, **39**, 2601–2611.

37 Y.-T. Tsai, H. Lin and M.-J. Lee, *Chem. Eng. J.*, 2011, **171**, 1367–1372.

38 T. Ito and F. Yoshida, *J. Chem. Eng. Data*, 1963, **8**, 315–320.

39 D. Painer and S. Lux, *Ind. Eng. Chem. Res.*, 2019, **58**, 1133–1141.

40 K. M. Kim, J. C. Kim, M. Cheong, J. S. Lee and Y. G. Kim, *Korean J. Chem. Eng.*, 1990, **7**, 259–268.

41 N. Iwasa, M. Terashita, M. Arai and N. Takezawa, *React. Kinet. Catal. Lett.*, 2001, **74**, 93–98.

42 G. Braca, A. M. R. Galletti, G. Sbrana, M. Lami and M. Marchionna, *J. Mol. Catal. A: Chem.*, 1995, **95**, 19–26.

43 D. M. Monti, M. S. Wainwright, D. L. Trimm and N. W. Cant, *Ind. Eng. Chem. Prod. Res. Dev.*, 1985, **24**, 397–401.

44 J. Wu, G. Liu, Q. Liu, Y. Zhang, F. Ding and K. Wang, *Catalysts*, 2023, **13**, 1038.

45 G. Braca, A. M. R. Galletti, N. J. Laniyonu, G. Sbrana, E. Micheli, M. Di Girolamo and M. Marchionna, *Ind. Eng. Chem. Res.*, 1995, **34**, 2358–2363.

46 V. Haagen, J. Iser, M. Schörner, D. Weber, T. Franken, P. Wasserscheid and P. Schühle, *Green Chem.*, 2023, **25**, 2338–2348.

47 finanzen.net, DOLLARKURS | Euro Dollar Wechselkurs | EUR/USD, **https://www.finanzen.net/devisen/dollarkurs**, (accessed August 31, 2024).

48 Statista, Zuckerpreis bis Oktober 2024, **https://de.statista.com/statistik/daten/studie/434644/umfrage/zuckerpreis/**, (accessed August 25, 2024).

49 G. Towler, *Chemical Engineering Design: Principles, Practice and Economics of Plant and Process Design*, Elsevier, 3rd edn, 2021.

50 Statista, Wasserstoff, **https://de.statista.com/statistik/daten/studie/1195863/umfrage/produktionskosten-von-wasserstoff-nach-wasserstofftyp-in-deutschland/**, (accessed September 27, 2024).

51 S. Schemme, *Techno–economic Assessment of Processes for the Production of Fuels from H_2 and CO_2*, RWTH Aachen University, 2020.

52 M. Pérez-Fortes, J. C. Schöneberger, A. Boulamanti, G. Harrison and E. Tzimas, *Int. J. Hydrogen Energy*, 2016, **41**, 16444–16462.

53 Statista, Industriestrompreise inkl. Stromsteuer in Deutschland bis 2024, **https://de.statista.com/statistik/daten/studie/252029/umfrage/industriestrompreise-inkl-stromsteuer-in-deutschland/**, (accessed August 31, 2024).

54 C. Kumpidet, Friedrich-Alexander-Universität Erlangen-Nürnberg, *Transformation of biomass to platform chemicals using homogeneous polyoxometalate catalysts*, Friedrich-Alexander-Universität Erlangen-Nürnberg, 2020.

55 DBFZ, DBFZ Resource Database, **https://datalab.dbfz.de/resdb/maps?lang=en**, (accessed December 2, 2024).

56 European Biodiesel Board, EBB Statistical Report 2023, **https://ebb-eu.org/wp-content/uploads/2024/03/EBB_Statistical_Report2023-Final.pdf**, (accessed January 30, 2025).

57 L. R. Kumar, S. K. Yellapu, R. D. Tyagi and X. Zhang, *Bioresour. Technol.*, 2019, **293**, 122155.

58 S. V. Vassilev, D. Baxter, L. K. Andersen and C. G. Vassileva, *Fuel*, 2010, **89**, 913–933.

59 O. Greifenberg and A. Strohpreise, **https://www.strohpreis.de/**, (accessed December 11, 2024).

60 G. Skouteris, G. Rodriguez-Garcia, S. F. Reinecke and U. Hampel, *Bioresour. Technol.*, 2020, **312**, 123595.

61 X. Chen, J. Dhungel, S. P. Bhattarai, M. Torabi, L. Pendergast and D. J. Midmore, *J. Plant Ecol.*, 2011, **4**, 236–248.

62 S. Patkaew, S. DirekbusarakoKm, I. Hirono, S. Wuthisuthimethavee, S. Powtongsook and C. Pooljun, *Vet. World*, 2024, 50–58.

63 M. Holst, S. Aschbrenner, T. Smolinka, C. Voglstätter and G. Grimm, :Unav, *Fraunhofer-Gesellschaft*, 2021, preprint, DOI: 10.24406/PUBLICA-1318.

64 C. Kost, P. Müller, J. S. Schweiger, V. Fluri and J. Thomsen, *Stromgestehungskosten Erneuerbare Energien*, 2024.

65 EEG 2023 – Gesetz für den Ausbau erneuerbarer Energien, **https://www.gesetze-im-internet.de/eeg_2014/BJNR106610014.html**, (accessed December 11, 2024).

66 Sunfire, Pressurized Alkaline Electrolyzers (AEL), **https://sunfire.de/en/products/pressurized-alkaline-electrolyzers-ael/?_rsc=tsolk**, (accessed January 30, 2025).

67 E. Moioli, A. Wötzel and T. Schildhauer, *J. Cleaner Prod.*, 2022, **359**, 132071.

68 S. Verhelst, J. W. Turner, L. Sileghem and J. Vancoillie, *Prog. Energy Combust. Sci.*, 2019, **70**, 43–88.

69 M. Schölles and S. Kreidelmeyer, *Internationaler Energiepreisvergleich für die Industrie*, 2023.

70 K. Harris, R. G. Grim, Z. Huang and L. Tao, *Appl. Energy*, 2021, **303**, 117637.

71 DIN EN 16603-11:2020-02, DOI: 10.31030/3119848.

72 F. Bisotti, K. A. Hoff, A. Mathisen and J. Hovland, *Chem. Eng. Sci.*, 2024, **283**, 119416.

73 A. Molino, V. Larocca, S. Chianese and D. Musmarra, *Energies*, 2018, **11**, 811.

74 VärmlandsMetanol AB, Methanol from Wood Residues - an excellent multipurpose fossil free chemical!, **https://www.varmlandsmetanol.se/dokument/Folder%20VM%202021%20eng.pdf**, (accessed January 30, 2025).

75 Solution | Our Technology | Enerkem, **https://enerkem.com/solution/technology**, (accessed December 10, 2024).

76 methanex, Pricing – Current Posted Prices, **https://www.methanex.com/about-methanol/pricing/**, (accessed December 13, 2024).

77 S. Michailos, P. Sanderson, A. V. Zaragoza, S. McCord, K. Armstrong and P. Styring, *Methanol Worked Examples for the TEA and LCA Guidelines for CO_2 Utilization*, Global CO_2 Initiative@UM, 2018.